Metallogr. Microstruct. Anal. (2017) 6:425–432
DOI 10.1007/s13632-017-0381-6

TECHNICAL ARTICLE

Microstructure and Properties of Nitrogen-Alloyed Martensitic Stainless Steel

S. Chenna Krishna[1] · N. K. Karthick[1] · Abhay K. Jha[1] · Bhanu Pant[1] · P. V. Venkitakrishnan[1]

Received: 22 May 2017 / Revised: 9 August 2017 / Accepted: 11 August 2017 / Published online: 1 September 2017

Abstract The microstructure and properties of a nitrogen-alloyed martensitic stainless steel in different heat treatment conditions were investigated in the present work. Hardness, compressive strength and microstructure were evaluated in the different heat treatment conditions, viz. hardening, cryo treatment and tempering. In the hardened condition, the microstructure consists of lath martensite, retained austenite, $M_{23}C_6$ carbides and MX-type carbonitrides. The typical compressive yield strength (CYS) and hardness in hardened condition were 1835 MPa and 610 VHN, respectively. After cryo treatment at −80 °C and tempering (500 °C), the hardness and CYS increased to 1936 MPa and 686 VHN, respectively. The increase in CYS and hardness is attributed to the formation of fine Mo_2C and Cr_2N particles.

Keywords Hardness · Retained austenite · Heat treatment · Nitrogen-alloyed martensitic stainless steel · Strength

Introduction

Bearing is a mechanical component which consists of inner race, outer race, rolling elements and a separator. Bearing is designed to reduce friction, support loads, guide moving parts and sustain severe static as well as cyclic loads in difficult environments [1]. Therefore, a bearing material should possess properties such as high hardness, dimensional stability, high fatigue strength, low coefficient of friction and good corrosion resistance [1, 2]. Steels are suitable for such application because of their availability in many forms (wire, rod and bar) and better mechanical properties [1, 3–5]. One of the prime requirements for such steels is martensitic structure with distributed carbides. Evolution of steels for bearing applications started with a high-carbon steel AISI 52100 with nominal composition of Fe-1.5Cr-1C (wt.%). This steel can be hardened and tempered to achieve different levels of hardness [6]. The corrosion resistance of steel is poor due to low amount of chromium (1.5%) and formation of M_7C_3 and $M_{23}C_6$ which leads to further depletion of chromium in the matrix [1]. Some of the steels with higher concentrations of alloying elements have been developed to (i) withstand high temperature (M50, M50 NiL, M62) [1], (ii) improve corrosion resistance (440C, Cronidur 30, XD15NW, 13Cr-SS) [2, 7, 8], (iii) very high hardness (CRU80) [3] and (iv) microstructure with fine carbides (Fe-17Cr-0.43C-0.17N, Cronidur 30, XD15NW, N360) [2, 9, 10]. To increase the corrosion resistant and toughness of bearing steel, AISI 440C was designed with high chromium [7, 8]. A 17 wt.% of Cr imparts corrosion resistance and combines with carbon to form M_7C_3 and $M_{23}C_6$ carbides [8]. Carbide banding and the presence of large M_7C_3 carbides in 440C are reported to have adverse effect on the fatigue life of bearing and corrosion resistance [8, 11]. These carbides can be avoided by reduction in carbon content in the steel. To reduce carbon content without deterioration in hardness and corrosion resistance, nitrogen was added which paved way for a new type of stainless steels [4, 9]. These steels are reported to have fine carbides and also result in uniform distribution of the carbides. Nitrogen imparts solid solution strengthening, improves pitting resistance and induces secondary hardening by the formation of nitrides. Despite the fact that nitrogen is beneficial, it is difficult to dissolve

✉ S. Chenna Krishna
chenna.sk@gmail.com

[1] Materials and Mechanical Entity, Vikram Sarabhai Space Centre, Trivandrum 695022, India

in martensite due to low solubility and special techniques are employed to melt such steels [12–14]. It was done by partial replacement of carbon by nitrogen (up to 0.22 wt.%) and minor additions of niobium and vanadium. Stainless steel with these modifications was melted through air induction melting (AIM) and electro-slag remelting (ESR). The corrosion behavior of the steel in different heat treatment conditions was studied and compared with 440C steel [11]. In the present study, mechanical properties and microstructure of the steel in different heat treatment conditions are investigated.

Experimental Procedure

The material used in the study was a 150 mm diameter × 250 mm length annealed bar melted through AIM and ESR. The cast ingot was homogenized and processed through forging (1080–950 °C). The forged bar was annealed at 850 °C for 6 h and air cooled to soften the steel. The chemical composition of the steel is given in Table 1. A slice cut from the bar was hot worked (forging and rolling) in the temperature range (1080–950 °C) to produce a plate of 12 mm thickness. Samples cut from plate were subjected to hardening, cryo treatment and tempering. Hardening was performed in the temperature range of 900–1100 °C for 0.5 h and oil quenched, followed by cryo treatment at −80 °C for 2 h and warming to room temperature in a cryo-chamber. The time delay between hardening and cryo treatment was maintained within 24 h. This was followed by tempering at different temperatures (180–700 °C) for 2 h. The details of heat treatment performed are given in Table 2. The hardness of the heat treated samples was measured using a Vickers hardness tester with a test load and dwell time of 20 kgf and 10 s, respectively. An average of five readings is reported here. Compression testing was performed on 6 mm diameter and 9 mm length specimens. Three independent compression tests were conducted, and average values are reported. Samples for metallography were prepared by mechanical polishing using different grades of emery papers, alumina paste and diamond paste. Polished samples were etched with acetic glyceregia (15 cc HCL + 10 cc HNO_3 + 10 cc acetic acid + 2 drops glycerine). Duly etched samples were examined under an optical microscope and scanning electron microscope. Thin foils for transmission electron microscopy (TEM) were prepared by polishing 300 μm from either side. Disk of 3 mm diameter was punched out from 100 μm thin foils and twin-jet polished using a solution of 10% perchloric acid and 90% ethanol at room temperature with a voltage of 30 V. Thin foils were examined under a transmission electron microscope (JEOL) equipped with energy dispersive x-ray spectroscopy (EDS) operated at 200 kV. X-ray diffraction (XRD) analysis was performed using a Philips x-ray diffraction instrument with Cu (K_α) x-ray source to determine dislocation density. Thermodynamic calculations were done using Thermo-Calc software.

Table 1 Chemical composition of the steel

Elements	C	Cr	Mo	Nb	V	N	Si	Fe
wt. %	0.435	15.99	1.73	0.14	0.20	0.224	0.21	Bal.

Results

Thermodynamic Calculations

Thermo-Calc software was used for the calculation of phase equilibria in the martensitic stainless steel with carbon and nitrogen. Figure 1 shows the phase diagram of

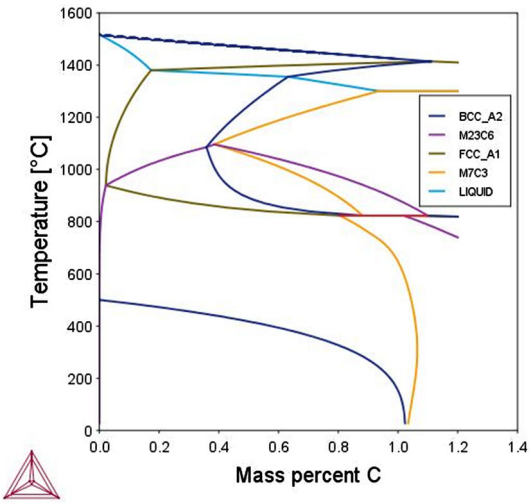

Fig. 1 Fe-Cr-C phase diagram: 17% Cr isopleth

Table 2 Heat treatment cycles employed

Identification	Heat treatment cycle
H1050	Holding at 1050 °C for 0.5 h and oil quenching
H1050 + C-80 + T180	H1050 + −80 °C for 2 h and air warming + 180 °C for 2 h and air cooling
H1050 + C-80 + T500	H1050 + −80 °C for 2 h and air warming + 500 °C for 2 h and air cooling
H1050 + C-80 + T550	H1050 + −80 °C for 2 h and air warming + 550 °C for 2 h and air cooling

the Fe-17Cr-XC system with a carbon content as a function of temperature. The equilibrium phases in the temperature range of 950–1100 °C are austenite, $M_{23}C_6$ and M_7C_3. Upon quenching, the austenite will transform to martensite with small quantity of retained austenite. Carbides ($M_{23}C_6$, M_7C_3) will be retained after quenching. It is reported that M_7C_3 carbides are deleterious to fatigue life of the bearings and lead to premature failure [15, 16]. It is possible to minimize these carbides by proper selection of the carbon content. The stable phases at 1050 °C for carbon content less than 0.5 wt.% are austenite and $M_{23}C_6$. However, to achieve a hardness of 58 HRc which is material requirement for bearings, the carbon should be higher than 0.6 wt.% in the martensite matrix [8]. One of the ways to achieve the hardness and also minimize M_7C_3 carbides is to replace some amount of carbon with nitrogen. Based on these calculations, steel with following composition was designed: Fe-0.43C-0.22N-17Cr (wt.%) with minor additions of V and Nb.

Figure 2 shows the amount of phases as a function of temperature in two martensitic stainless steels. The phases in the 440C steel in the temperature range of 200–1600 °C are bcc, fcc, $M_{23}C_6$ and M_7C_3 carbides (Fig. 2a). The volume fraction of M_7C_3 in the 440C steel at 1000 and 1050 °C was 0.06 and 0.08, respectively. In the present steel, the stable phases at the temperature range of 900–1100 °C are fcc and $M_{23}C_6$, as shown in Fig. 2b. At 1050 °C, the volume fraction of austenite and $M_{23}C_6$ is 0.981 and 0.019, respectively.

Hardness

Figure 3 shows the influence of hardening and tempering temperature on the hardness of the steel. The hardness of the steel increased with an increase in the hardening temperature in the range of 900–1050 °C (Fig. 3a). Maximum and minimum hardness of 610 and 526 VHN was observed at 1050 and 900 °C, respectively. Based on the hardness trend, hardening temperature of 1050 °C was chosen and further heat treatment was performed on these samples. The effect of tempering temperature on the hardened samples is shown in Fig. 3b. The hardness decreased (590–540 VHN) with an increase in the tempering temperature in the range of 180–350 °C. An increase in

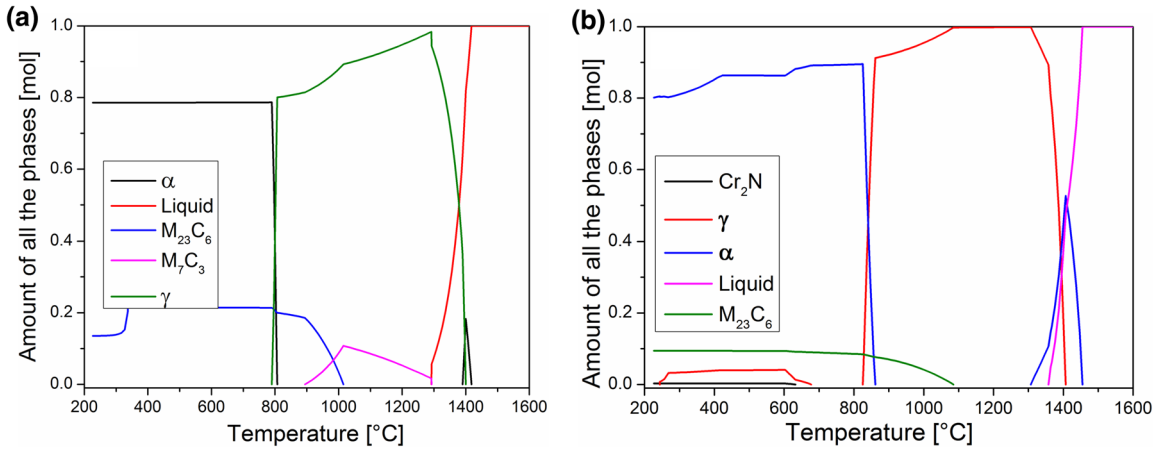

Fig. 2 Phase fraction of all the phases as a function of temperature in: (**a**) 440C steel and (**b**) present steel (Thermo-Calc)

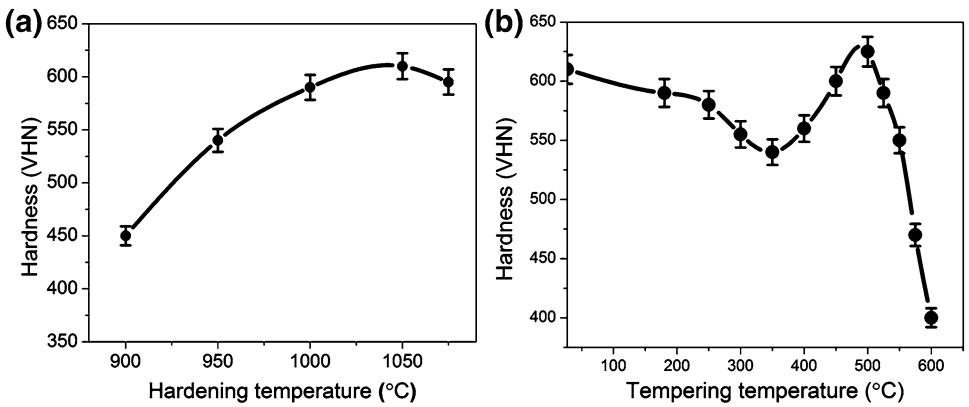

Fig. 3 Effect of heat treatment on the hardness of the steel (**a**) hardening and (**b**) tempering of the samples hardened at 1050 °C for 0.5 h and oil quenched

hardness (560–625 VHN) was observed in the temperature range of 400–500 °C. Beyond 500 °C, a drop in hardness was observed and a minimum hardness of 400 VHN was observed for the sample tempered at 600 °C.

The hardness of the steel subjected to different heat treatments is shown in Fig. 4. In hardened condition, the steel showed a hardness of 610 VHN. After the cryo treatment and tempering at 180 °C, minor decrease in hardness (600 VHN) was observed. Tempering at 500 °C resulted in maximum hardness of 686 VHN. The hardness decreased to 576 VHN after tempering at 550 °C. The reason for change in hardness after hardening and tempering will be explained with the aid of XRD measurement and TEM analysis.

Compressive Strength

Steels for bearings in hardened and tempered condition possess high strength and are not ductile [1]. The ductility for such steel is very low (1–4%), and it is difficult to obtain consistent and meaningful tensile data. Large scatter in tensile data was observed for the present steel, and tensile ductility was less than 3%. It was also reported that the compressive yield strength (CYS) is a better indication of the load capacity [3]. Therefore, compression test was performed on the heat treated samples. The effect of heat treatment on the compressive strength of the steel is shown in Fig. 5. The CYS of the steel in hardened condition was 1835 MPa. Cryo treatment and tempering at 180 °C has led to marginal decrease in CYS with a value of 1825 MPa. Maximum CYS of 1936 MPa was observed after tempering at 500 °C. Tempering at 550 °C caused a decrease in CYS with a value of 1824 MPa.

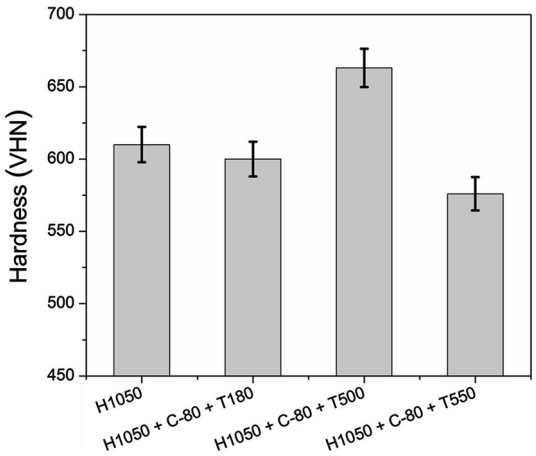

Fig. 4 Hardness of the steel in different heat treatment conditions (hardening, cryo treatment and tempering)

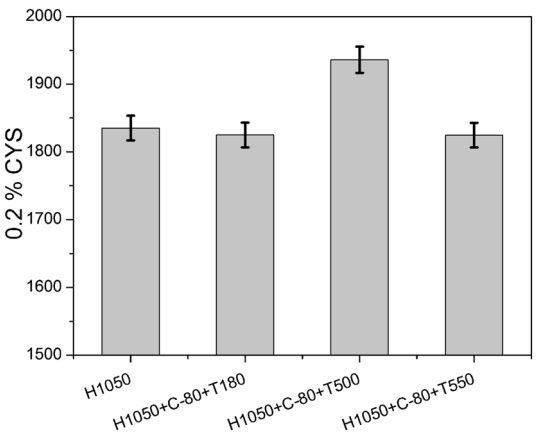

Fig. 5 Compressive yield strength of the steel in different heat treatment conditions

Microscopy

The optical micrograph of the steel in the hardened condition is shown in Fig. 6. The microstructure consists of primary $M_{23}C_6$ carbides well distributed in the martensite matrix. Large carbides (M_7C_3) and carbide banding typically reported in high-carbon steels [8, 17] were not observed in the present steel. Cryo treatment and tempering did not show any significant change in the microstructure that can be observed under optical microscope. The hardened microstructure consists of lath martensite and primary $M_{23}C_6$ carbides with chemical formula $(FeCrMo)_{23}C_6$ (Fig. 7a). The average size of the carbides was measured to be 0.4 μm. However, at certain locations very fine carbides were observed as indicated by arrows. Figure 7b shows the microstructure of the cryo treated and tempered (500 °C) sample which consists of tempered martensite and secondary carbides. The volume fraction of carbides is higher compared to H1050 due to the formation of new carbides. Growth of the fine carbides in H1050 sample (Fig. 7a) was

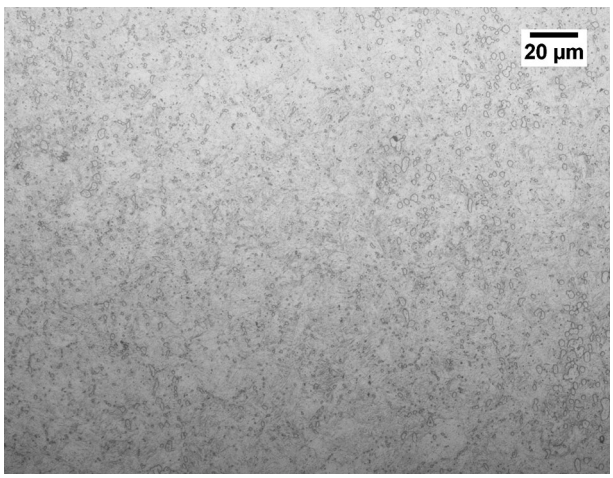

Fig. 6 Optical micrographs of the steel in hardened condition etched with acetic glyceregia

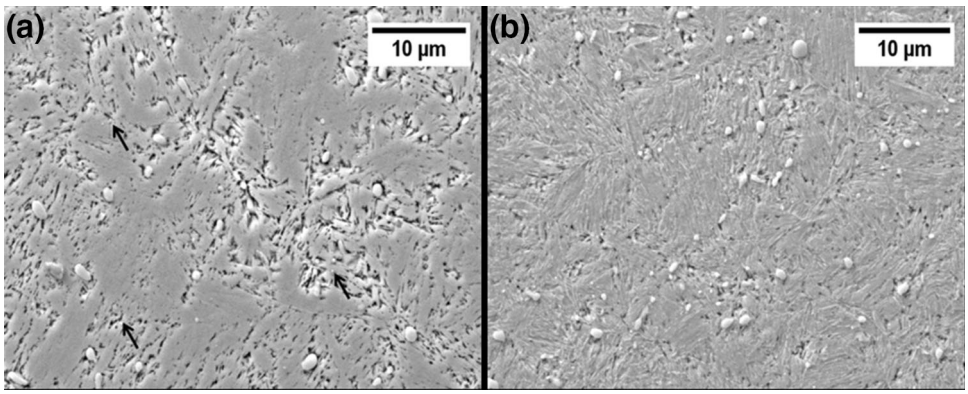

Fig. 7 SEM micrographs of the steel in two heat treatment conditions: (**a**) H1050 (arrows pointing fine carbides in the martensite matrix) and (**b**) H1050 + C-80 + T500

also observed. The average size of the carbides was 0.52 μm.

Discussion

The stable phases in the steel over the temperature range of 1000–1050 °C are bcc, fcc and $M_{23}C_6$. The phase fraction of the phases varies with the temperature as shown in Fig. 2b. The microstructure of the steel quenched from above temperature range will consist of martensite (bcc), $M_{23}C_6$ and retained austenite (fcc). The variation in the hardness with the hardening temperature (Fig. 3a) is mainly due to changes in the phase fraction of austenite and $M_{23}C_6$. The volume fraction of carbides gradually decreases with the hardening temperature which leads to increase in the carbon content in the austenite. This carbon will be retained in the martensite after oil quenching from the hardening temperature. The carbon content of the austenite increases with the temperature from 0.09 wt.% (900 °C) and 0.32 wt.% (1050 °C). Small amount of $M_{23}C_6$ was observed in the hardened sample as shown in Fig. 6. Maximum hardness of 610 VHN observed at 1050 °C is due to higher content of carbon in austenite (0.32 wt.%) which significantly contributes to hardness [18, 19]. The marginal reduction in hardness at 1075 °C may be attributed to growth of prior austenite grain size which leads to increase in the lath size and higher content of retained austenite after quenching as reported in martensitic stainless steels [20, 21].

The hardness of the H1050 sample after tempering in the temperature range of 180–600 °C showed a decreasing trend up to 350 °C and increased in the temperature range of 350–500 °C. Tempering beyond 500 °C led to decrease in the hardness (Fig. 3b). Decrease in the hardness in the temperature range of 180–350 °C is attributed to the formation of transition carbides and reduction in the internal stresses and dislocation density (8.12×10^{14} m^{-2}) compared to H1050 sample.

The dislocation density was determined from the XRD measurement using the following formula [22]:

$$\text{Dislocation density } (\rho) = 14.4\left(\frac{\varepsilon^2}{b^2}\right) \quad (1)$$

where b is the burgers vector of dislocation (0.253 nm) and ε is the local strain obtained by Hall–Williamson method.

Increase in the hardness over the range (350–500 °C) is attributed to secondary hardening due to the formation of Cr_2N and Mo_2C particles in martensite matrix. In the temperature range of 500–600 °C, the reduction in hardness may be attributed to increase in austenite content due to the formation of reversed austenite [23, 24] and coarsening of the carbides [21].

Properties of the Steel in Four Heat Treatment Conditions

Hardened (H1050)

The high hardness (610 VHN) and CYS (1835 MPa) of the steel in the hardened condition is due to solid solution strengthening (Cr, C and N) and dispersion strengthening (carbides). Martensite in steels (Fe-C) is associated with higher hardness compared to ferrite and austenite due to dislocated structure and internal stresses [19]. Increase in the carbon content of such steels (Fe-C) leads to improvement in the hardness [18]. Steels with Fe-1.5Cr-1C, Fe-17Cr-1C and Fe-15Cr-0.6C are reported to have high hardness (54-62 HRC) [1, 8, 20]. In the present steel, carbon (0.435 wt.%) and nitrogen (0.22 wt.%) contribute significantly to the solid solution strengthening. On the other hand, $M_{23}C_6$ and MX particles impart strength by dispersion hardening. The microstructure of H1050 sample comprises of martensite, retained austenite, $M_{23}C_6$ carbides and MX-type carbonitrides as shown in Figs. 7 and 8. Retained austenite was observed as thin film between the martensite lath (Fig. 8a). Spherical MX-type carbonitrides and coarse carbides ($M_{23}C_6$) are shown in Fig. 8b and c,

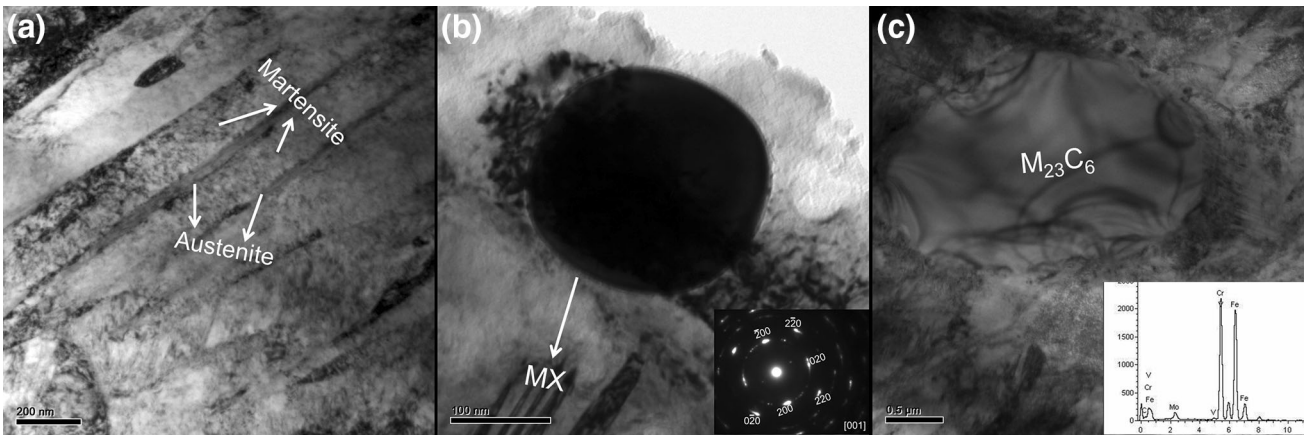

Fig. 8 Bright-field TEM images of the H1050 sample: (**a**) martensite and retained austenite, (**b**) MX-type carbonitrides and (**c**) $M_{23}C_6$ carbides

respectively. The chemical formula of the MX and $M_{23}C_6$ was (NbVCr)(C,N) and $(FeCrMo)_{23}C_6$, respectively. The dislocation density of hardened sample was calculated to be 2×10^{15} m^{-2}. All these factors contribute to high hardness and CYS.

Tempered at 180 °C (H1050 + C-80 + T180)

The microstructural changes after tempering at 180 °C are reduction in the dislocation density and formation of the transition carbides. Diffusion of carbon and nitrogen in the martensite matrix is expected to occur in the temperature of 180–550 °C [25, 26]. Dislocation lines act as diffusion path for the interstitial elements like carbon and nitrogen. Different types of carbides have been reported at 180 °C in medium- and high-carbon steels [26]. The fine transition carbides that formed in the steel after tempering are shown in Fig. 9a. These transition carbides will lead to depletion of carbon in the martensite matrix which results in decrease in hardness. The minor reduction in hardness and CYS of T180 sample compared to H1050 is due to combined effect of decrease in the dislocation density (8.2×10^{14} m^{-2}) and formation of transition carbides.

Tempered at 500 °C (H1050 + C-80 + T500)

Formation of fine nano-sized particles is the microstructural change observed in the T500 sample. In addition to $M_{23}C_6$ carbides (Fig. 9a), two types of particles observed in T500 sample were spherical (Mo_2C) and rod shaped (Cr_2N) as shown in Fig. 9b. Average size of the Mo_2C particles was 4 nm, and width of Cr_2N was 35 nm. Similar type of observations was reported after tempering at 500 °C in Fe-16Cr-0.16N-0.4C [10], Cronidur 30 [9], XDN15W [2], 15Cr-5Ni-1W-1Mo [27]. Minor increase in austenite content is also expected to occur compared to H1050 at tempering temperature of 500 °C as predicted from Thermo-Calc calculations (Fig. 2b). An increase in 76 VHN and 101 MPa in hardness and CYS, respectively, in T500 compared to H1050 is attributed to secondary hardening due to the formation of Mo_2C and Cr_2N particles.

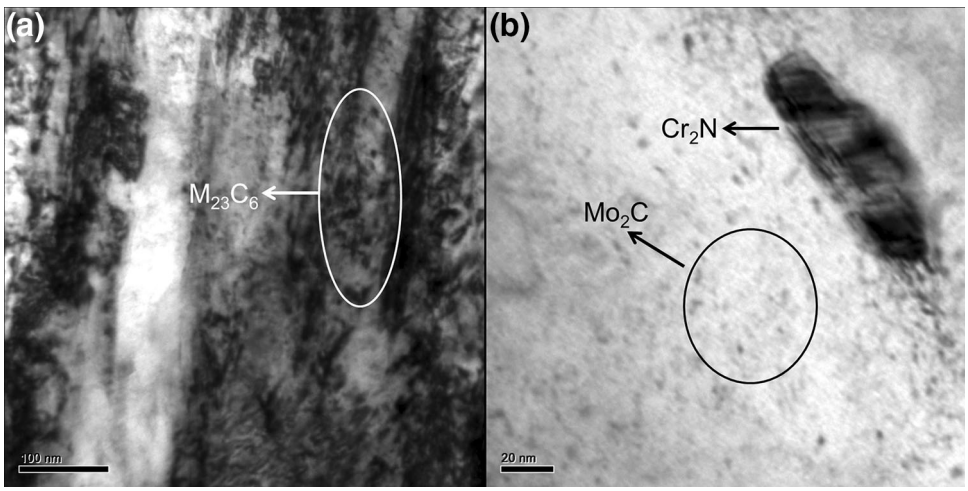

Fig. 9 Bright-field TEM micrographs of the steel: (**a**) H1050 + C-80 + T180 and (**b**) H1050 + C-80 + T500

Tempered at 550 °C (H1050 + C-80 + T550)

Reduction in CYS and hardness after tempering at 550 °C is mainly due to increase in the austenite content (Fig. 2a) and decrease in the dislocation density. Austenite content was reported to increase with tempering temperature (500–700 °C) in martensitic stainless steel due to the formation of the reversed austenite [24, 28, 29]. The dislocation density of the T550 was 2.72×10^{14} m^{-2} which is lower than H1050.

Conclusions

Through the limited studies conducted on the nitrogen-alloyed martensitic stainless steel in different heat treatment conditions, the conclusions drawn are: The microstructure of the steel in the H1050 condition comprises of lath martensite, retained austenite, primary carbides ($M_{23}C_6$) and carbonitrides (MX). These microstructural features resulted in hardness and compressive yield strength of 610 VHN and 1835 MPa, respectively. Tempering at 180 °C (H1050 + C-80 + T180) led to minor reduction in the mechanical properties due to decrease in the dislocation density and formation of transition carbides. Improvement in hardness (686 VHN) and compressive yield strength (1936 MPa) after tempering at 500 °C (H1050 + C-80 + T500) is mainly attributed to secondary hardening by the formation of Mo_2C and Cr_2N particles.

Acknowledgments The authors would like to thank their colleagues at Material Characterization Division (VSSC) for their support in mechanical testing of the samples. The authors would like to express sincere gratitude to the Director, VSSC for his kind permission to publish this work.

References

1. H.K.D.H. Bhadeshia, Progress in materials science steels for bearings. Prog. Mater. Sci. **57**, 268–435 (2012). doi:10.1016/j.pmatsci.2011.06.002
2. D. Girodin, L. Manes, J.-Y. Moraux, J.-M. de Monicault, Characterisation of The XD15N high nitrogen martensitic stainless steel for aerospace bearing, aerospace. *4th International Conference on Launcher Technology "Space Launcher Liquid Propulsion"* (2002)
3. K. Clemons, C. Lorraine, G. Salgado, A. Taylor, J. Ogren, P. Umin et al., Effects of heat treatments on steels for bearing applications. J. Mater. Eng. Perform. **16**, 592–596 (2007). doi:10.1007/s11665-007-9075-6
4. N. Mitamura, Y. Murakami, Development of NSJ2 bearing steel. NSK J. Motion Control. **8**, 27–34 (2000)
5. D.W. Hetzner, W. Van Geertruyden, Crystallography and metallography of carbides in high alloy steels. Mater. Charact. **59**, 825–841 (2008). doi:10.1016/j.matchar.2007.07.005
6. C.A. Stickels, Carbide refining heat treatments for 52100 bearing steel. Metall. Trans. **5**, 865–874 (1974). doi:10.1007/BF02643140
7. J.R. Yang, T.H. Yu, C.H. Wang, Martensitic transformations in AISI 440C stainless steel. Mater. Sci. Eng. A **438–440**, 276–280 (2006). doi:10.1016/j.msea.2006.02.098
8. S.C. Krishna, K.T. Tharian, K.V.A. Chakravarthi, A.K. Jha, B. Pant, Heat treatment and thermo-mechanical treatment to modify carbide banding in AISI 440C steel: a case study. Metallogr. Microstruct. Anal. **5**, 108–115 (2016). doi:10.1007/s13632-016-0266-0
9. W. Trojahn, E. Streit, H.A. Chin, D. Ehlert, Progress in bearing performance of advanced nitrogen alloyed stainless steel, Cronidur 30, in *Bear. Steels into 21st Century* (ASTM International, 1998)
10. S.C. Krishna, N.K. Gangwar, A.K. Jha, B. Pant, K.M. George, Effect of heat treatment on the microstructure and hardness of 17Cr–0.17N–0.43C–1.7Mo martensitic stainless steel. J. Mater. Eng. Perform. **24**, 1656–1662 (2015). doi:10.1007/s11665-015-1431-3
11. R. Ghosh, S. Chenna Krishna, A. Venugopal, P. Ramesh Narayanan, A.K. Jha, P. Ramkumar, et al., Corrosion and nanomechanical behaviors of 16.3Cr–0.22N–0.43C–1.73Mo martensitic stainless steel. Corros. Sci. Technol. **15**, 281–289 (2016)
12. S. Ma, S. Chu, Z. Zhang, Y. Qiu, Principle and practice of high nitrogen steel melting by blowing ammonia gas. J. Iron. Steel Res. Int. **17**, 6–9 (2010). doi:10.1016/S1006-706X(10)60050-7
13. L. Sun, J. Li, L. Zhang, S. Yang, Y. Chen, Production of nitrogen-bearing stainless steel by injecting nitrogen gas. J. Iron. Steel Res. Int. **18**, 7–11 (2011). doi:10.1016/S1006-706X(11)60109-X
14. M.A. Ragen, D.L. Anthony, R.F. Spitzer, A comparison of the mechanical and physical properties of contemporary and new alloys for aerospace bearing applications, in *Bear. Steel Technol.* (ASTM International, 2002)
15. R.J. Parker, E.N. Bamberger, Effect of carbide distribution on rolling-element fatigue life of AMS 5749 (1983)
16. P.K. Adishesha, Effect of steel making and processing parameters on carbide banding in commercially produced ASTM A-295 52100 bearing steel. ASTM Spec. Tech. Publ. **1419**, 27–46 (2002)
17. J.D. Verhoeven, A review of microsegregation induced banding phenomena in steels. J. Mater. Eng. Perform. **9**, 286–296 (2000). doi:10.1361/105994900770345935
18. R.A. Grange, C.R. Hribal, L.F. Porter, Hardness of tempered martensite in carbon and low-alloy steels. Metall. Trans. A **8**, 1775–1785 (1977). doi:10.1007/BF02646882
19. G. Krauss, Martensite in steel: strength and structure. Mater. Sci. Eng. A **273–275**, 40–57 (1999). doi:10.1016/S0921-5093(99)00288-9
20. L.D. Barlow, M. Du Toit, Effect of austenitizing heat treatment on the microstructure and hardness of martensitic stainless steel AISI 420. J. Mater. Eng. Perform. **21**, 1327–1336 (2011). doi:10.1007/s11665-011-0043-9
21. A.N. Isfahany, H. Saghafian, G. Borhani, The effect of heat treatment on mechanical properties and corrosion behavior of AISI420 martensitic stainless steel. J. Alloys Compd. **509**, 3931–3936 (2011). doi:10.1016/j.jallcom.2010.12.174
22. K. Nakashima, M. Suzuki, Y. Futamura, T. Tsuchiyama, S. Takaki, Limit of dislocation density and dislocation strengthening in iron. Mater. Sci. Forum **503–504**, 627–632 (2006). doi:10.4028/www.scientific.net/MSF.503-504.627
23. W. Jiang, K. Zhao, D. Ye, J. Li, Z. Li, J. Su, Effect of heat treatment on reversed austenite in Cr15 super martensitic stainless steel. J. Iron. Steel Res. Int. **20**, 61–65 (2013). doi:10.1016/S1006-706X(13)60099-0
24. D. Ye, J. Li, W. Jiang, J. Su, K. Zhao, Formation of reversed austenite in high temperature tempering process and its effect on mechanical properties of Cr15 super martensitic stainless steel

alloyed with copper. Steel Res. Int. **84**, 395–401 (2013). doi:10.1002/srin.201200105
25. V.G. Gavriljuk, Nitrogen in iron and steel. ISIJ Int. **36**, 738–745 (1996). doi:10.2355/isijinternational.36.738
26. G. Krauss, Deformation and fracture in martensitic carbon steels tempered at low temperatures. Metall. Mater. Trans. B **32**, 205–221 (2001). doi:10.1007/s11663-001-0044-4
27. S.C. Krishna, N.K. Gangwar, A.K. Jha, B. Pant, K.M. George, Microstructure and properties of 15Cr–5Ni–1Mo–1W martensitic stainless steel. Steel Res. Int. **86**, 51–57 (2015). doi:10.1002/srin.201400035
28. B. Qin, Z.Y. Wang, Q.S. Sun, Effect of tempering temperature on properties of 00Cr16Ni5Mo stainless steel. Mater. Charact. **59**, 1096–1100 (2008). doi:10.1016/j.matchar.2007.08.025
29. M. Al Dawood, I.S. El Mahallawi, M.E. Abd El Azim, M.R. El Koussy, Thermal aging of 16Cr–5Ni–1Mo stainless steel part 1—microstructural analysis. Mater. Sci. Technol. **20**, 363–369 (2004). doi:10.1179/026708304225011135